International Journal of Mass Spectrometry 456 (2020) 116396

Contents lists available at ScienceDirect

International Journal of Mass Spectrometry

journal homepage: www.elsevier.com/locate/ijms

Gold nanostructures - assisted laser desorption/ionization mass spectrometry for kidney cancer blood serum biomarker screening

Adrian Arendowski [a, *], Krzysztof Ossoliński [b], Joanna Nizioł [a], Tomasz Ruman [a]

[a] Faculty of Chemistry, Rzeszów University of Technology, 6 Powstańców Warszawy Ave, 35-959, Rzeszów, Poland
[b] Department of Urology, John Paul II Hospital, Grunwaldzka 4 St, 36-100, Kolbuszowa, Poland

ARTICLE INFO

Article history:
Received 20 June 2020
Received in revised form
13 July 2020
Accepted 20 July 2020
Available online 27 July 2020

Keywords:
Cancer biomarker
Gold nanoparticles
Kidney Cancer
Laser desorption/ionization
Mass spectrometry
Renal cell carcinoma

ABSTRACT

Kidney cancer is a disease diagnosed annually in 400,000 people for which there are no specific biomarkers found to date. It is therefore important to search for new chemical compounds to detect cancer state. Laser desorption/ionization mass spectrometry on gold nanoparticle-enhanced target (AuNPET) method was used in this work for rapid metabolic analysis of blood serum of fifty patients with renal cancer. Comparison with data from sera of fifty healthy volunteers allowed discovering potential biomarkers of renal cell carcinoma (RCC). Statistical analysis of *m/z* values that had the greatest impact on group differentiation allowed. Database search allowed providing assignment of signals for the most promising eleven features among them: dihydrouracil, creatinine, glutamine, tyrosine, 2,3-diaminosalicylic acid, 3-hydroxykynurenine, 2-hydroxylauroylcarnitine, melatonin glucuronide, palmitoyl glucuronide, triglyceride(52:4) or phosphatidylcholine(42:0). This work demonstrate that the differences in metabolite profiles in serum of kidney cancer patients and that of healthy subjects could be identified by gold nanostructures LDI MS – based metabolomics and exploited as metabolic serum markers for the early detection of kidney cancer.

1. Introduction

According to GLOBOCAN, in 2018, there were approximately 400000 new cases of kidney cancer and more than 175000 deaths due to this disease [1]. More than 80% of adult kidney cancers are renal cell carcinomas (RCCs) [2], which are a heterogeneous group of tumors classified by WHO into several subtypes: clear cell (ccRCC), chromophobe RCC (cRCC) and papillary RCC (pRCC), medullary and collecting duct, and other unclassified subtypes [3]. RCC can develop for a long time without clinical symptoms, whereby more than half of the cases are diagnosed incidentally, usually by medical imaging methods, and up to 20% of patients have metastases at the time of diagnosis [4]. Thus early detection of renal cell carcinoma is crucial for its treatment and it is important to develop new procedures for early detection of renal cell carcinoma, among them the most important are based on specific chemical compounds called biomarkers that might indicate a development of tumor.

Proteomic approach predominates in current strategies of cancer biomarker search and although several RCC protein biomarkers have been proposed, but they suffer from low sensitivity and specificity [5]. Cancer is a disease that alters cell metabolism, so it seems that the appropriate approach will be the metabolic profiling of kidney tissue and bioliquids such as serum and urine [6].

The most frequently used techniques for metabolomic profiling of kidney cancer have been: LC-MS (liquid chromatography mass spectrometry) [7,8], GC-MS (gas chromatography mass spectrometry) often used with pre-column derivatization [9] and ^{1}H NMR (proton nuclear magnetic resonance) [10–12]. It should be mentioned that mass spectrometry (MS) is the most commonly used family of methods in cancer biomarker research mainly due to its high resolution and sensitivity compared to other methods. Kidney cancer is considered a metabolomic disease, therefore a growing number of studies focus on profiling of biofluids such as plasma [12] and serum [13,14] can be found in literature.

Among the various MS techniques of ionization, matrix-assisted

Abbreviations: AUC, area under the curve; AuNPET, gold nanoparticle-enhanced target; LDI, laser desorption/ionization; MS, mass spectrometry; OPLS-DA, orthogonal projections to latent structures discriminant analysis; PCA, principal component analysis; PLS-DA, partial least squares; discriminant analysis, RCC; renal cell carcinoma, ROC; receiver operating characteristic, SALDI; surface-assisted laser desorption/ionization, sPLS-DA; sparse partial least squares, discriminant analysis.

* Corresponding author.
E-mail address: adrian@arendowski.hub.pl (A. Arendowski).

https://doi.org/10.1016/j.ijms.2020.116396
1387-3806/

laser desorption/ionization (MALDI) technique deserves special attention. Due to the soft ionization process, high mass determination accuracy and very high sensitivity over a wide mass range, this method is among the best choices for biological material analysis. MALDI MS method has already been used as a tool for tumor marker research [15,16] including peptide and protein profiling for renal cell carcinoma [17].

However, MALDI spectra contain a high chemical background below *m/z* 1000 due to the use of organic matrices. For small molecules, surface-assisted laser desorption/ionization (SALDI) [18] solutions are generally better suited. As literature search prove, gold nanostructures are among the most frequently used for laser MS. Some of the recent applications of gold nanostructures in LDI MS include nanoflowers of Au@MnO previously applied for analysis of small and also large molecules of cancer cell lysates [19,20]. Kuo group has used multilayer thin films of gold nanoparticles with a thickness of 2.7 μm for the quantitative determination of bone biomarker - hydroxyproline in blood of patients suffering from osteoporosis [21]. AuNPs assisted LDI-MS imaging was reported for metabolites, including neurotransmitters, fatty acids and nucleobases, detected from mouse brain tissue [22,23]. Our group presented the advantages of gold-nanoparticle enhanced target (AuNPET) for laser desorption/ionization mass spectrometry analysis and imaging of low molecular weight compounds of different polarity in complex biological mixtures [24–28], also in kidney tissue [29]. Compared to commonly used MALDI MS our method has been proven to produce much lower chemical background, allows much more precise internal calibration and is better for medium and low polar compounds.

This work demonstrate the capabilities of AuNPET LDI MS method for rapid metabolic screening of fifty serum samples of patients with diagnosed renal cell carcinoma and statistical comparison with control group of fifty serum samples of healthy volunteers in order to discovering of new candidates for biomarkers.

2. Experimental

2.1. Participants

Serum samples were obtained from fifty patients with diagnosed kidney cancer. Control was fifty serum samples from healthy volunteers, for which the presence of renal tumors had been excluded by abdominal ultrasound. Specimens and clinical data from patients involved in the study were collected with written consent. Patient who agreed to participate in the study donated 10 ml of blood according to standard medical procedure. All experiments were performed in compliance with the local laws and institutional guidelines (Rzeszów University of Technology biological material guidelines). Research protocol was approved by the local bioethics committee at the University of Rzeszów (Poland). Patient characteristics are provided in Table 1.

2.2. Materials & methods

Chloro(trimethylphosphite)gold(I) of 97+% purity (Aldrich) was used for nanoparticle synthesis. The pyridine–borane complex (BH_3:py) used was at ~8 M borane concentration (Aldrich). All solvents was of HPLC quality and were purchased from Sigma-Aldrich (Poland), except for 18 MΩ water which was produced locally. Magnetic stainless steel plate of H17 grade was made locally and used with Bruker NALDI adapter.

2.3. Preparation of AuNPET target

The gold nanoparticle-covered target was prepared similarly to the one described in our recent publication [30]. Stainless steel plate of 35x45 mm size was inserted into a large Petri dish containing acetonitrile (50 mL) and dissolved chloro(-trimethylphosphite)gold(I) (25 mg). To this solution, 8M BH_3:py complex in pyridine (173 μL) was added. After 48 h of reaction, target plate was washed several times with acetonitrile, wiped with cotton wool ball and washed three times with acetonitrile and deionized water.

2.4. Sample preparation

Serum samples obtained from patients were immediately frozen and stored at −60 °C. Prior to measurements, an unfreezing step was performed in room temperature, followed by 500-times dilution with ultrapure water. Volumes of 0.5 μL of urine solutions were placed directly on target plate, air dried and inserted into MS apparatus for measurements.

2.5. LDI MS experiment

Laser desorption/ionization mass spectrometry experiments were performed using Bruker Autoflex Speed Time-of-Flight mass spectrometer equipped with a SmartBeam II laser (355 nm) in positive-ion reflectron mode. Measurement range was *m/z* 80–2000, suppression was turned on for *m/z* lower than 79. Laser impulse energy was approximately 100–190 μJ and laser repetition rate 1000 Hz. Number of laser shots was 20 000 (4x5000 shots) for each sample spot. The first accelerating voltage was held at 19 kV and the second ion source voltage at 16.7 kV. Reflector voltages used were 21 kV (the first) and 9.55 kV (the second). The data was calibrated with FlexAnalysis (version 3.3) using enhanced cubic calibration model and analyzed with mMass 5.5.0-open source program [31]. Mass calibration was performed using internal standards (gold ions and clusters from Au^+ to Au_5^+). Reproducibility was tested by measuring triplicates and comparing signals intensities for *m/z* values for ions: Au^+ to Au_5^+ for ten cancer and ten normal samples. All intensities were within 20% of mean value.

2.6. Data analysis

Database search of chemical compounds were carried out using a custom made program for Human Metabolome Database (HMDB) [32] and LipidMaps [33] search. Theoretical *m/z* values were confirmed by using ChemCalc program available online [34]. Statistical analysis of results was performed with the use of MetaboAnalyst 4.0 service [35]. Data was normalized by sum, cube root transformed and default Pareto scaling was used. For creating receiver operating characteristic (ROC) curve random forests has been chosen as classification method and RandomForest was selected as feature ranking method.

3. Results and discussion

The aim of the research was to find metabolites present in serum that could be biomarkers for kidney cancer. For this purpose, serum from fifty people with diagnosed kidney cancer and fifty healthy volunteers was analyzed using laser desorption/ionization mass spectrometry method based on gold nanoparticles surface target (AuNPET). Spectra for randomly chosen five cancer and five control samples are shown in Fig. 1. Obtained spectra from patients and controls were compared with the aid of MetaboAnalyst 4.0 [35].

In order to estimate the degree of influence of method-related spectral data over sample-related data statistical analysis was performed. Principal component analysis (PCA), Orthogonal-

Table 1
Clinical characteristics of patients.

		Patients
Total		50
Age (years)		35–89
Mean		62
Sex	Male	30
	Female	20
Stage (T)	T1	33
	T2	3
	T3	10
	T4	1
	undefined	3
Nodes (N)	N0	46
	N1	1
	undefined	3
Metastases (M)	M0	42
	M1	5
	undefined	3
Grade (Fuhrman)	I	7
	II	17
	III	13
	IV	2
	undefined	11

Orthogonal Projections to Latent Structures Discriminant Analysis (OPLS-DA), Partial Least Squares - Discriminant Analysis (PLS-DA) and Sparse Partial Least Squares - Discriminant Analysis (sPLS-DA) statistical methods implemented in MetaboAnalyst web service were used. In case of domination of method-related data or signals, statistical analysis could not provide clear enough separation of studied samples.

Analyzing Fig. 2, containing results of statistical analysis of blood serum mass spectrometry data, can be concluded that only OPLS-DA score plot (Fig. 2C) presents completely separated groups. The other three of used statistical methods: PCA (Fig. 2A and B), PLS-DA (Fig. 2D–F) and sPLS-DA (Fig. 2G and H), did not allow for complete separation of cancer patients and control group. These results are not unexpected as cancer and control samples are very similar from molecular point of view and usually complete separation in PCA is not visible. Furthermore, studied cancer group originates from patients with cancer of various stages and grades.

Based on PLS-DA, fold-change, t-tests and random forest classification statistical methods, *m/z* values that had the greatest impact on group separation were obtained. Mass features were assigned with the aid of HMDB [32] which allowed listing of 11 potential biomarkers shown in Table 2, which also includes a VIP score, p-value and fold change between healthy controls and kidney cancer for each of them. Random Forest classification method allowed the Out-of-bag (OOB) error to be determined at the 0.18 level, correctly classifying healthy people to the control group in 80%, and people with diagnosed kidney cancer as patients in 84%, based on all signals present in mass spectra.

Fig. 3 presents box plots and ROC curves for each of eleven *m/z* values. The largest area under the curve (AUC) was recorded for *m/z* 398.23015 and is 0.728, while the smallest for *m/z* 457.2586 is 0.588. Ten of the metabolites (creatinine, glutamine, tyrosine, 2,3-diaminosalicylic acid, 3-hydroxykynurenine, 2-hydroxylauroyl carnitine, melatonin glucuronide, palmitoyl glucuronide, triglyceride(52:4) and phosphatidylcholine(42:0)) shown in Table 2 show up-regulation in serum samples from patients with kidney cancer, only one has higher intensities in the control samples.

Dihydrouracil was the only compound showing down-regulation in patients' serum (Fig. 3A). It is an intermediate in the reaction of uracil degradation catalyzed by dihydropyrimidine dehydrogenase. Studies on the activity of dihydropyrimidine dehydrogenase in patients with RCC showed its reduced activity of this enzyme in the study group compared to the control [36], which may explain the down-regulation in our samples.

The first *m/z* value for which up-regulation in cancer (Fig. 3B) was observed - 152.0213 - was assigned to potassium adduct of creatinine, a breakdown product of creatine phosphate in muscle.

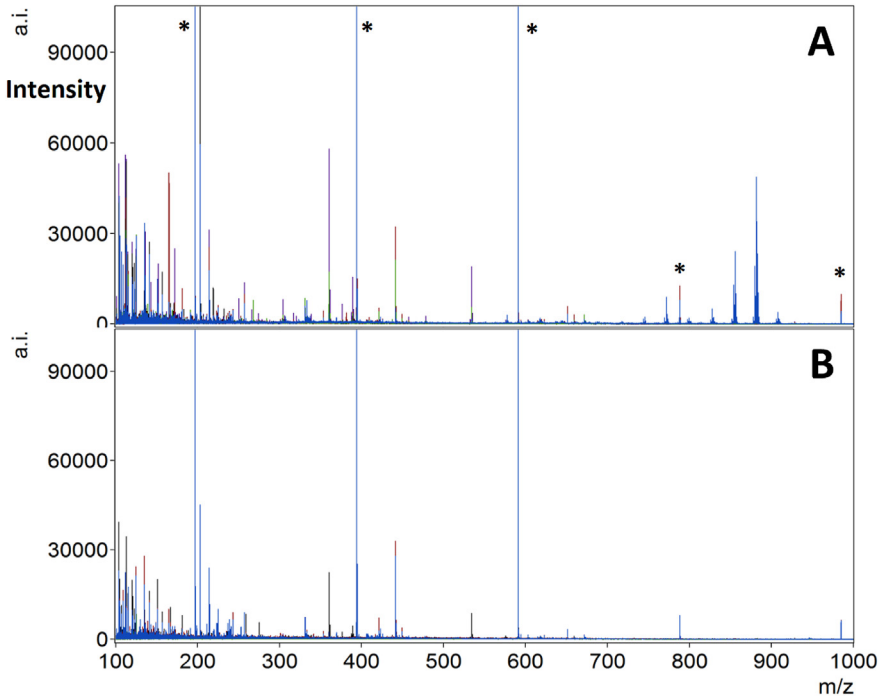

Fig. 1. Examples of AuNPET LDI MS spectra for five randomly chosen cancer (A) and control (B) sera. Asterisks marks gold ions used for calibration. (For interpretation of the references to colour in this figure legend, the reader is referred to the Web version of this article.)

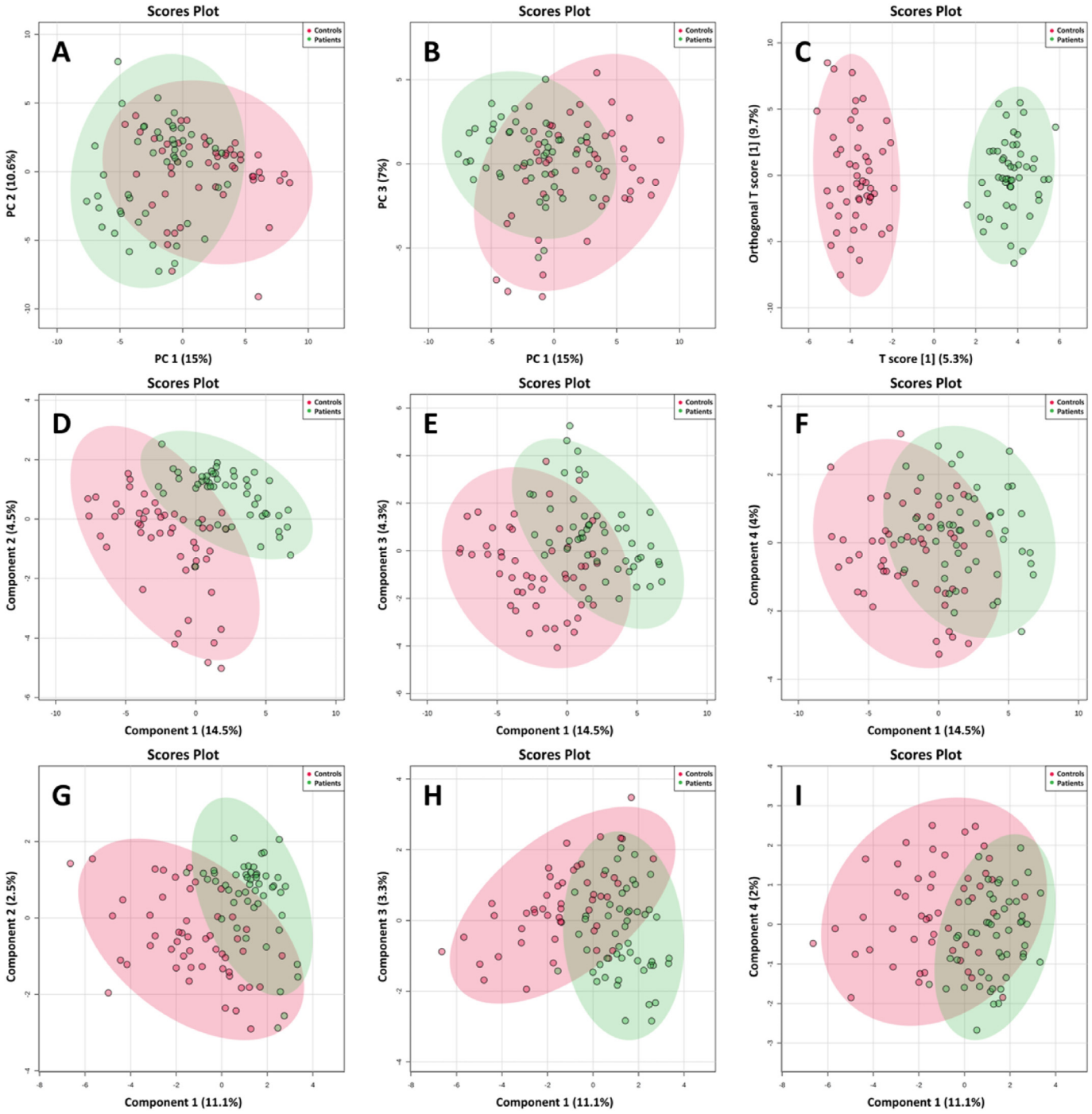

Fig. 2. Graphical representation of statistical analysis of MS data: PCA – component 1 vs 2 (A) and vs 3 (B), OPLS-DA (C), PLS-DA – component 1 vs 2 (D), vs 3 (E), vs 4 (F) and sPLS-DA component 1 vs 2 (G), vs 3 (H) and vs 4 (I). Red area represents data for controls while green for cancer patients.

Increased blood creatinine levels are observed with chronic renal failure [37]. This is due to damage to the functioning nephrons, which can also occur with the development of a kidney tumor. Higher creatinine levels were also seen in pancreatic cancer [38]. Two metabolites with higher intensities in cancer samples are amino acids – glutamine and tyrosine. Up-regulation of serum glutamine can be explained by the fact that some cancers, such as renal cell carcinoma require exogenous glutamine for growth and have reprogrammed glutamine metabolism [39]. Glutamine has already been previously described as a potential biomarker for RCC [40]. Tyrosine was detected in the serum of patients with kidney cancer but either its level measured by NMR did not show a difference from the control [11] or decreased as during LC-MS analysis [8]. Another compound putatively identified as 2,3-diamino salicylic acid is a metabolite normally found in human blood and urine [32] but has not yet been described as a biomarker of renal cell carcinoma.

Hydroxykynurenine for which the observed area under the curve is 0.645 (Fig. 3F) is a metabolite in the kynurenine pathway, the major route of tryptophan degradation in mammals. Researchers

Table 2
List of ions and compounds found by statistical analysis of mass spectra.

Metabolite	Ion formula	Experimental *m/z*	Calculated *m/z*	Δ*m/z* [ppm]	Controls	Patients	VIP	P-Value	FC[a]	Figure
Dihydrouracil	$[C_4H_6N_2O_2+H]^+$	115.0518	115.0502	13.9	+	−	1.39	5.3E-3	1.23	3A
Creatinine	$[C_4H_7N_3O + K]^+$	152.0213	152.0221	−5.3	−	+	1.38	1.4E-3	0.69	3B
Glutamine	$[C_5H_{10}N_2O_3+K]^+$	185.0312	185.0323	−5.9	−	+	0.70	1.5E-4	0.82	3C
Tyrosine	$[C_9H_{11}NO_3+Na]^+$	204.0615	204.0631	−7.8	−	+	1.40	6.0E-5	0.53	3D
2,3-Diaminosalicylic acid	$[C_7H_8N_2O_3+K]^+$	207.0192	207.0167	12.1	−	+	1.63	2.6E-6	0.51	3E
3-Hydroxykynurenine	$[C_{10}H_{12}N_2O_4+Na]^+$	247.0705	247.0689	6.5	−	+	0.78	1.7E-2	0.51	3F
2-Hydroxylauroylcarnitine	$[C_{19}H_{37}NO_5+K]^+$	398.2302	398.2303	−0.3	−	+	0.98	1.4E-3	0.48	3G
Melatonin glucuronide	$[C_{19}H_{24}N_2O_8+H]^+$	409.1582	409.1605	−5.6	−	+	1.03	3.3E-3	0.42	3H
Palmitoyl glucuronide	$[C_{22}H_{42}O_7+K]^+$	457.2586	457.2562	5.2	−	+	0.82	1.1E-2	0.55	3I
TG(52:4)	$[C_{55}H_{100}O_5+K]^+$	879.7081	879.7202	−13.8	−	+	1.88	1.4E-4	0.08	3J
PC(42:0)	$[C_{50}H_{102}NO_7P + Na]^+$	882.7269	882.7286	−1.9	−	+	1.85	2.1E-4	0.07	3K

[a] Fold change between controls and cancer samples.

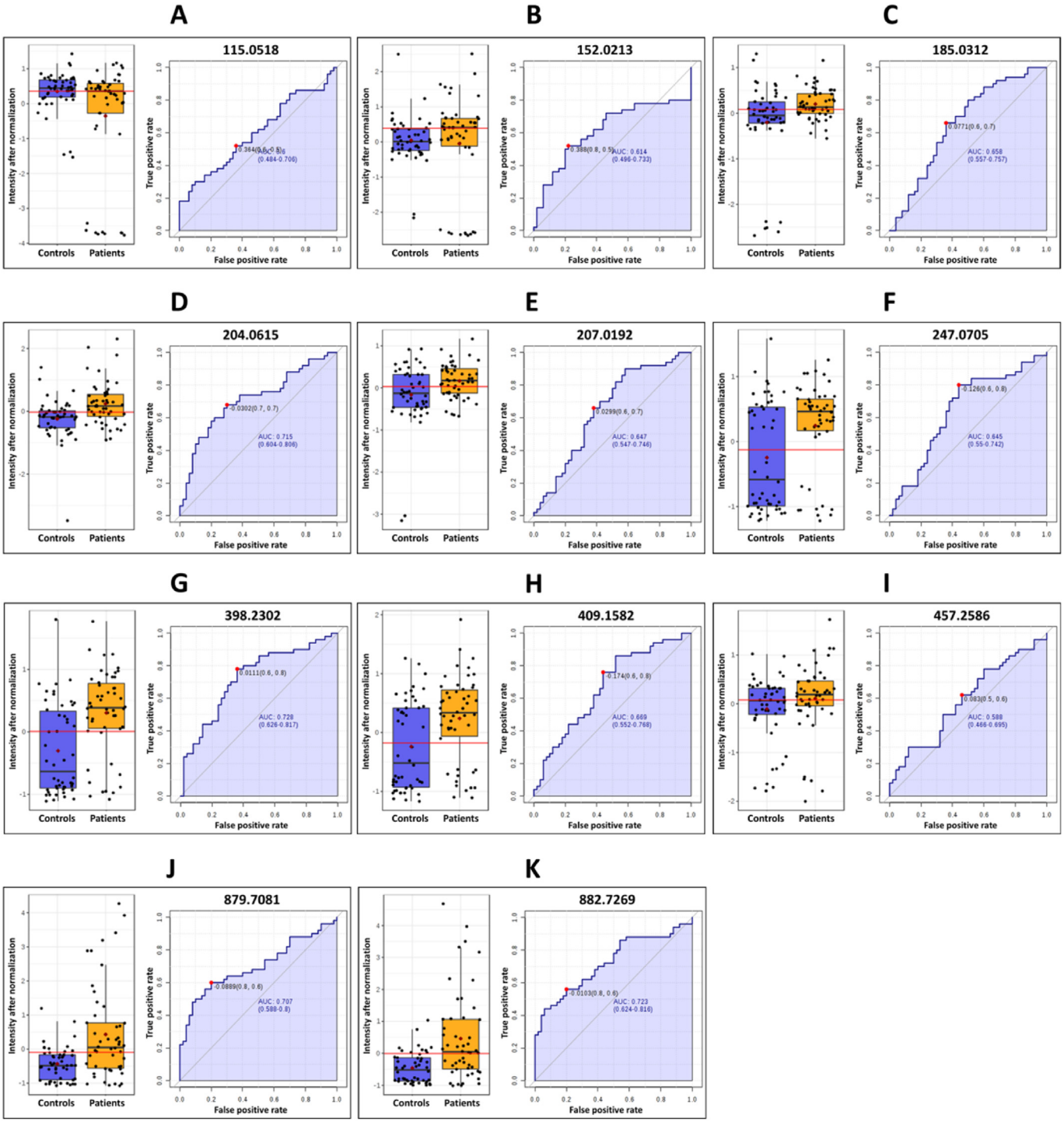

Fig. 3. Box plots and ROC curves for *m/z* values: 115.0518 (A), 152.0213 (B), 185.0312 (C), 204.0615 (D), 207.0192 (E), 247.0705 (F), 398.2302 (G), 409.1582 (H), 457.2586 (I), 879.7081 (J) and 882.7269 (K) respectively. Vertical axes of box plots are intensities after normalization.

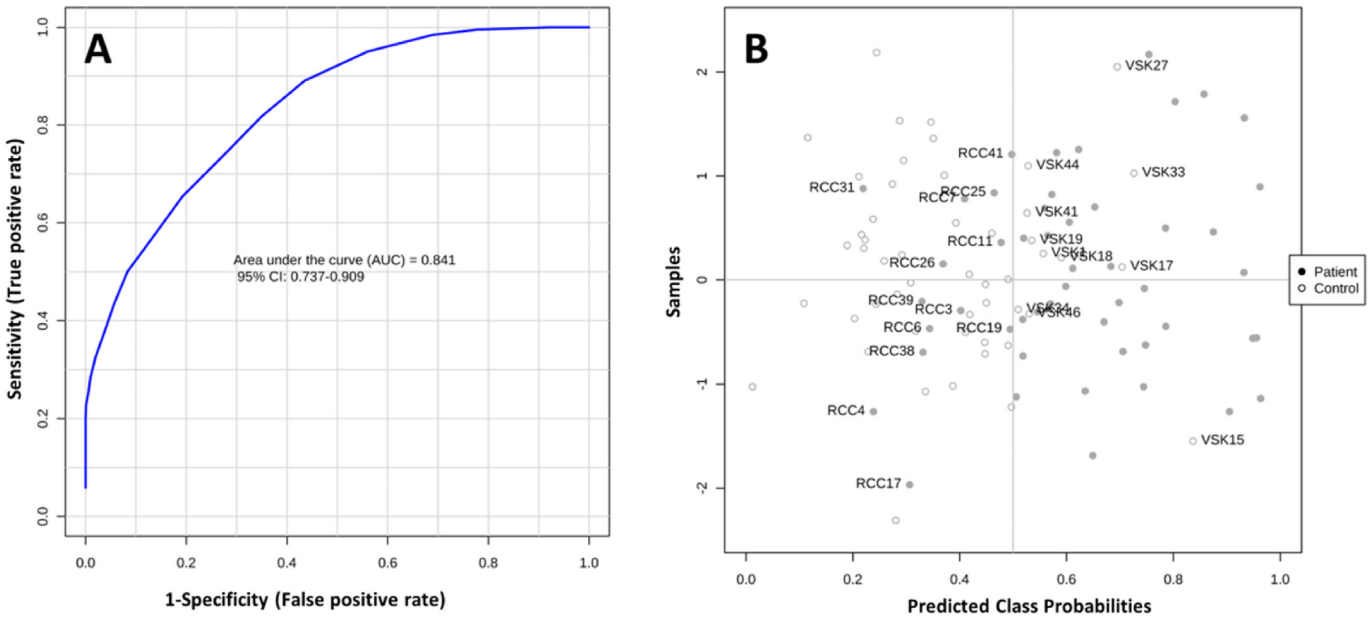

Fig. 4. Multivariate ROC curve based exploratory analysis based on 11-mass feature intensity data processed in MetaboAnalyst service, showing area under the curve (A) and predicted class probabilities for each sample with labels for samples classified to the wrong groups (B). RCC are cancer and VSK – control samples.

have observed a high incidence of abnormal excretion of tryptophan metabolites in kidney cancer, indicating changes in renal function due to the presence of a tumor [41], but so far no changes in the level of 3-hydroxykynurenine in the blood of RCC patients have been observed.

Metabolite whose potassium adduct has been attributed m/z 398.2302 is 2-hydroxylauroylcarnitine. This potential biomarker for RCC with up-regulation has largest area under the curve equal 0.728 (Fig. 3G). The presence of acyl carnitines in higher concentrations than in the control group was previously found in the tissues and urine of patients with kidney cancer [40,42]. A possible explanation for these changes is that cancer cells require more energy from fatty acid β-oxidation, which acyl carnitines are intermediates [43]. Another two metabolites are compounds belonging to the group glucuronides – melatonin glucuronide and palmitoyl glucuronide with AUC 0.669 (Figs. 3H) and 0.588 (Fig. 3I) respectively, and showing higher intensities among cancer samples compared to controls. Melatonin glucuronide is a metabolite of melatonin, naturally occurring compound found in animals [32], but not yet described as a potential RCC biomarker. Palmitoyl glucuronide is a common liver metabolite of palmitic acid which is excreted by kidneys [44] found by our group in kidney tissue but showing down-regulation in the cancerous area [45].

Two lipid compounds were also found to be potential biomarkers - triglyceride TG(52:4) and phosphatidylcholine PC(42:0). TG presence in renal cell carcinoma is critical for sustained tumorigenesis but tumor cell viability is incompletely understood [46]. Studies have shown kidney tumor tissue contains twice the amount of phosphatidylcholines compared to normal [47].

For all eleven mass features intensity table was created and then receiver operating characteristic (ROC) analysis was performed in MetaboAnalyst. The results of the analysis are presented in Fig. 4. Area under the curve for the proposed biomarkers was found to be 0.841 (Fig. 4) thus they have high diagnostic accuracy to distinguish patients with kidney cancer from the healthy people from control group. Predicted class probabilities for each sample shown in Fig. 4B were made on the basis of AUC. Cross-validation allowed for correct classification 37 samples to be qualified as originating from patients with kidney cancer, which gives 74% efficiency (sensitivity of test) and 39 samples as derived from healthy volunteers, giving 78% correctness (specificity). Positive predictive value (PPV) of this test is 77%, negative predictive value (NPV) is 75%, and accuracy is equal to 76%.

Based on our recent publications [29,40] it can be concluded that the change of lipid content is an important feature of RCC. Accuracy of the model based on the two lipids proposed in this article as potential biomarkers - triglyceride(52:4) and phosphatidylcholine(42:0) was tested. The area under the ROC curve plotted for these two compounds was 0.717 (Supplementary materials S1). A number of 32 samples were correctly certified as both true positive and true negative using this model (Supplementary materials S2) that gives 76% accuracy.

4. Conclusions

Laser desorption/ionization mass spectrometry with gold nanoparticle-enhanced SALDI-type target was used for rapid analysis of serum from 50 patients with diagnosed kidney cancer and 50 healthy volunteers. Methodology allowed identification of up- and downregulated eleven compounds that could potentially serve as renal cancer biomarkers such as: dihydrouracil, creatinine, glutamine, tyrosine, 2,3-diaminosalicylic acid, L-3-hydroxykynurenine, 2-hydroxylauroylcarnitine, melatonin glucuronide, palmitoyl glucuronide, triglyceride(52:4) or phosphatidylcholine(42:0). Multivariate ROC analysis proposed biomarkers gave an area under the curve equal to 0.841, and correct classification of patients and healthy people (accuracy) at 76%. Statistical analysis allowed to distinguish the study group from the control.

CRediT authorship contribution statement

Adrian Arendowski: Formal analysis, Investigation, Writing - original draft, Visualization, Funding acquisition. **Krzysztof Ossoliński:** Resources. **Joanna Nizioł:** Methodology, Resources, Writing - review & editing. **Tomasz Ruman:** Conceptualization, Methodology, Writing - review & editing, Supervision.

Declaration of competing interest

The authors declare that they have no known competing financial interests or personal relationships that could have appeared to influence the work reported in this paper.

Acknowledgments

Scientific work funded by Ministry of Science and Higher Education Republic of Poland from the budget for science in the years 2016–2020 as a research project within the program "Diamond Grant" (project no. 0184/DIA/2016/45). Mr Dominik Ruman is acknowledged for creating MS search engine of chemical compounds.

Appendix A. Supplementary data

Supplementary data to this article can be found online at https://doi.org/10.1016/j.ijms.2020.116396.

References

[1] F. Bray, J. Ferlay, I. Soerjomataram, R.L. Siegel, L.A. Torre, A. Jemal, Global cancer statistics 2018: GLOBOCAN estimates of incidence and mortality worldwide for 36 cancers in 185 countries, CA Canc. J. Clin. 68 (2018) 394–424, https://doi.org/10.3322/caac.21492.
[2] W.-H. Chow, L.M. Dong, S.S. Devesa, Epidemiology and risk factors for kidney cancer, Nat. Rev. Urol. 7 (2010) 245–257, https://doi.org/10.1038/nrurol.2010.46.
[3] H. Moch, An overview of renal cell cancer: pathology and genetics, Semin. Canc. Biol. 23 (2013) 3–9, https://doi.org/10.1016/j.semcancer.2012.06.006.
[4] U. Capitanio, F. Montorsi, Renal cancer, Lancet 387 (2016) 894–906, https://doi.org/10.1016/S0140-6736(15)00046-X.
[5] A.L. Pastore, G. Palleschi, L. Silvestri, D. Moschese, S. Ricci, V. Petrozza, A. Carbone, A. Di Carlo, Serum and urine biomarkers for human renal cell carcinoma, Dis. Markers 2015 (2015) 1–9, https://doi.org/10.1155/2015/251403.
[6] M.S. Monteiro, M. Carvalho, M. de Lourdes Bastos, P.G. de Pinho, Biomarkers in renal cell carcinoma: a metabolomics approach, Metabolomics 10 (2014) 1210–1222, https://doi.org/10.1007/s11306-014-0659-5.
[7] L. Lin, Z. Huang, Y. Gao, Y. Chen, W. Hang, J. Xing, X. Yan, LC-MS-based serum metabolic profiling for genitourinary cancer classification and cancer type-specific biomarker discovery, Proteomics 12 (2012) 2238–2246, https://doi.org/10.1002/pmic.201200016.
[8] L. Lin, Z. Huang, Y. Gao, X. Yan, J. Xing, W. Hang, LC-MS based serum metabonomic analysis for renal cell carcinoma diagnosis, staging, and biomarker discovery, J. Proteome Res. 10 (2011) 1396–1405, https://doi.org/10.1021/pr101161u.
[9] B.B. Misra, R.P. Upadhayay, L.A. Cox, M. Olivier, Optimized GC–MS metabolomics for the analysis of kidney tissue metabolites, Metabolomics 14 (2018) 75, https://doi.org/10.1007/s11306-018-1373-5.
[10] H. Gao, B. Dong, J. Jia, H. Zhu, C. Diao, Z. Yan, Y. Huang, X. Li, Application of ex vivo 1H NMR metabonomics to the characterization and possible detection of renal cell carcinoma metastases, J. Canc. Res. Clin. Oncol. 138 (2012) 753–761, https://doi.org/10.1007/s00432-011-1134-6.
[11] A.N. Zira, S.E. Theocharis, D. Mitropoulos, V. Migdalis, E. Mikros, 1 H NMR metabonomic analysis in renal cell carcinoma: a possible diagnostic tool, J. Proteome Res. 9 (2010) 4038–4044, https://doi.org/10.1021/pr100226m.
[12] F. Süllentrop, D. Moka, S. Neubauer, G. Haupt, U. Engelmann, J. Hahn, H. Schicha, 31P NMR spectroscopy of blood plasma: determination and quantification of phospholipid classes in patients with renal cell carcinoma, NMR Biomed. 15 (2002) 60–68, https://doi.org/10.1002/nbm.758.
[13] L. Lin, Q. Yu, X. Yan, W. Hang, J. Zheng, J. Xing, B. Huang, Direct infusion mass spectrometry or liquid chromatography mass spectrometry for human metabonomics? A serum metabonomic study of kidney cancer, Analyst 135 (2010) 2970–2978, https://doi.org/10.1039/C0AN00265H.
[14] F. Zhang, X. Ma, H. Li, G. Guo, P. Li, H. Li, L. Gu, X. Li, L. Chen, X. Zhang, The predictive and prognostic values of serum amino acid levels for clear cell renal cell carcinoma, Urol. Oncol. Semin. Orig. Investig. 35 (2017) 392–400, https://doi.org/10.1016/j.urolonc.2017.01.004.
[15] H. Bateson, S. Saleem, P.M. Loadman, C.W. Sutton, Use of matrix-assisted laser desorption/ionisation mass spectrometry in cancer research, J. Pharmacol. Toxicol. Methods 64 (2011) 197–206, https://doi.org/10.1016/j.vascn.2011.04.003.
[16] M.A. Merlos Rodrigo, O. Zitka, S. Krizkova, A. Moulick, V. Adam, R. Kizek, MALDI-TOF MS as evolving cancer diagnostic tool: a review, J. Pharmaceut. Biomed. Anal. 95 (2014) 245–255, https://doi.org/10.1016/j.jpba.2014.03.007.
[17] E. Gianazza, C. Chinello, V. Mainini, M. Cazzaniga, V. Squeo, G. Albo, S. Signorini, S.S. Di Pierro, S. Ferrero, S. Nicolardi, Y.E.M. van der Burgt, A.M. Deelder, F. Magni, Alterations of the serum peptidome in renal cell carcinoma discriminating benign and malignant kidney tumors, J. Proteom. 76 (2012) 125–140, https://doi.org/10.1016/j.jprot.2012.07.032.
[18] J. Sunner, E. Dratz, Y.-C. Chen, Graphite surface-assisted laser desorption/ionization time-of-flight mass spectrometry of peptides and proteins from liquid solutions, Anal. Chem. 67 (1995) 4335–4342, https://doi.org/10.1021/ac00119a021.
[19] I. Ocsoy, B. Gulbakan, M.I. Shukoor, X. Xiong, T. Chen, D.H. Powell, W. Tan, Aptamer-conjugated multifunctional nanoflowers as a platform for targeting, capture, and detection in laser desorption ionization mass spectrometry, ACS Nano 7 (2013) 417–427, https://doi.org/10.1021/nn304458m.
[20] H.N. Abdelhamid, H.-F. Wu, Gold nanoparticles assisted laser desorption/ionization mass spectrometry and applications: from simple molecules to intact cells, Anal. Bioanal. Chem. 408 (2016) 4485–4502, https://doi.org/10.1007/s00216-016-9374-6.
[21] X.-Y. Pan, C.-H. Chen, Y.-H. Chang, D.-Y. Wang, Y.-C. Lee, C.-C. Liou, Y.-X. Wang, C.-C. Hu, T.-R. Kuo, Osteoporosis risk assessment using multilayered gold-nanoparticle thin film via SALDI-MS measurement, Anal. Bioanal. Chem. 411 (2019) 2793–2802, https://doi.org/10.1007/s00216-019-01759-5.
[22] H.-W. Tang, M.Y.-M. Wong, W. Lam, Y.-C. Cheng, C.-M. Che, K.-M. Ng, Molecular histology analysis by matrix-assisted laser desorption/ionization imaging mass spectrometry using gold nanoparticles as matrix, Rapid Commun. Mass Spectrom. 25 (2011) 3690–3696, https://doi.org/10.1002/rcm.5281.
[23] H.N. Abdelhamid, Nanoparticle assisted laser desorption/ionization mass spectrometry for small molecule analytes, Microchim. Acta 185 (2018) 200, https://doi.org/10.1007/s00604-018-2687-8.
[24] J. Sekuła, J. Nizioł, M. Misiorek, P. Dec, A. Wrona, A. Arendowski, T. Ruman, Gold nanoparticle-enhanced target for MS analysis and imaging of harmful compounds in plant, animal tissue and on fingerprint, Anal. Chim. Acta 895 (2015) 45–53, https://doi.org/10.1016/j.aca.2015.09.003.
[25] A. Arendowski, T. Ruman, Laser desorption/ionisation mass spectrometry imaging of European yew (Taxus baccata) on gold nanoparticle-enhanced target, Phytochem. Anal. 28 (2017) 448–453, https://doi.org/10.1002/pca.2693.
[26] A. Arendowski, J. Szulc, J. Nizioł, B. Gutarowska, T. Ruman, Metabolic profiling of moulds with laser desorption/ionization mass spectrometry on gold nanoparticle enhanced target, Anal. Biochem. 549 (2018) 45–52, https://doi.org/10.1016/j.ab.2018.03.016.
[27] A. Arendowski, T. Ruman, Lysine detection and quantification by laser desorption/ionization mass spectrometry on gold nanoparticle-enhanced target, Anal. Methods 10 (2018) 5398–5405, https://doi.org/10.1039/C8AY01677A.
[28] K. Ossoliński, J. Nizioł, A. Arendowski, A. Ossolińska, T. Ossoliński, J. Kucharz, P. Wiechno, T. Ruman, Mass spectrometry-based metabolomic profiling of prostate cancer - a pilot study, J. Canc. Metastasis Treat. 5 (2019) 1, https://doi.org/10.20517/2394-4722.2018.63.
[29] J. Nizioł, K. Ossoliński, T. Ossoliński, A. Ossolińska, V. Bonifay, J. Sekuła, Z. Dobrowolski, J. Sunner, I. Beech, T. Ruman, Surface-transfer mass spectrometry imaging of renal tissue on gold nanoparticle enhanced target, Anal. Chem. 88 (2016) 7365–7371, https://doi.org/10.1021/acs.analchem.6b01859.
[30] J. Sekuła, J. Nizioł, W. Rode, T. Ruman, Gold nanoparticle-enhanced target (AuNPET) as universal solution for laser desorption/ionization mass spectrometry analysis and imaging of low molecular weight compounds, Anal. Chim. Acta 875 (2015) 61–72, https://doi.org/10.1016/j.aca.2015.01.046.
[31] T.H.J. Niedermeyer, M. Strohalm, mMass as a software tool for the annotation of cyclic peptide tandem mass spectra, PLoS One 7 (2012), e44913, https://doi.org/10.1371/journal.pone.0044913.
[32] D.S. Wishart, Y.D. Feunang, A. Marcu, A.C. Guo, K. Liang, R. Vázquez-Fresno, T. Sajed, D. Johnson, C. Li, N. Karu, Z. Sayeeda, E. Lo, N. Assempour, M. Berjanskii, S. Singhal, D. Arndt, Y. Liang, H. Badran, J. Grant, A. Serra-Cayuela, Y. Liu, R. Mandal, V. Neveu, A. Pon, C. Knox, M. Wilson, C. Manach, A. Scalbert, HMDB 4.0: the human metabolome database for 2018, Nucleic Acids Res. 46 (2018) D608–D617, https://doi.org/10.1093/nar/gkx1089.
[33] E. Fahy, M. Sud, D. Cotter, S. Subramaniam, LIPID MAPS online tools for lipid research, Nucleic Acids Res. 35 (2007) W606–W612, https://doi.org/10.1093/nar/gkm324.
[34] L. Patiny, A. Borel, ChemCalc: a building block for tomorrow's chemical infrastructure, J. Chem. Inf. Model. 53 (2013) 1223–1228.
[35] J. Chong, D.S. Wishart, J. Xia, Using MetaboAnalyst 4.0 for comprehensive and integrative metabolomics data analysis, Curr. Protoc. Bioinf. 68 (2019) e86, https://doi.org/10.1002/cpbi.86.
[36] Y. Mizutani, H. Wada, O. Yoshida, M. Fukushima, H. Nakanishi, M. Nakao, T. Miki, Significance of dihydropyrimidine dehydrogenase activity in renal cell carcinoma, Eur. J. Canc. 39 (2003) 541–547, https://doi.org/10.1016/S0959-8049(02)00730-X.
[37] T. Kikuchi, Y. Orita, A. Ando, H. Mikami, M. Fujii, A. Okada, H. Abe, Liquid-chromatographic determination of guanidino compounds in plasma and erythrocyte of normal persons and uremic patients, Clin. Chem. 27 (1981) 1899–1902.
[38] D. OuYang, J. Xu, H. Huang, Z. Chen, Metabolomic profiling of serum from human pancreatic cancer patients using 1H NMR spectroscopy and principal component analysis, Appl. Biochem. Biotechnol. 165 (2011) 148–154, https://doi.org/10.1007/s12010-011-9240-0.
[39] O.A. Aboud, S.L. Habib, J. Trott, B. Stewart, S. Liang, A.J. Chaudhari, J. Sutcliffe,

R.H. Weiss, Glutamine addiction in kidney cancer suppresses oxidative stress and can Be exploited for real-time imaging, Canc. Res. 77 (2017) 6746–6758, https://doi.org/10.1158/0008-5472.CAN-17-0930.
[40] J. Nizioł, V. Bonifay, K. Ossoliński, T. Ossoliński, A. Ossolińska, J. Sunner, I. Beech, A. Arendowski, T. Ruman, Metabolomic study of human tissue and urine in clear cell renal carcinoma by LC-HRMS and PLS-DA, Anal. Bioanal. Chem. 410 (2018) 3859–3869, https://doi.org/10.1007/s00216-018-1059-x.
[41] F.a.G. Teulings, H.A. Peters, W.C.J. Hop, W. Fokkens, W.G. Haije, H. Portengen, B. van der Werf-Messing, A new aspect of the urinary excretion of tryptophan metabolites in patients with cancer of the bladder, Int. J. Canc. 21 (1978) 140–146, https://doi.org/10.1002/ijc.2910210203.
[42] S. Ganti, S.L. Taylor, K. Kim, C.L. Hoppel, L. Guo, J. Yang, C. Evans, R.H. Weiss, Urinary acylcarnitines are altered in human kidney cancer, Int. J. Canc. 130 (2012) 2791–2800, https://doi.org/10.1002/ijc.26274.
[43] H.I. Wettersten, A.A. Hakimi, D. Morin, C. Bianchi, M.E. Johnstone, D.R. Donohoe, J.F. Trott, O.A. Aboud, S. Stirdivant, B. Neri, R. Wolfert, B. Stewart, R. Perego, J.J. Hsieh, R.H. Weiss, Grade-dependent metabolic reprogramming in kidney cancer revealed by combined proteomics and metabolomics analysis, Canc. Res. 75 (2015) 2541–2552, https://doi.org/10.1158/0008-5472.CAN-14-1703.
[44] R.S. Goldstein, Mechanisms of Injury in Renal Disease and Toxicity, CRC Press FL, USA, 1994.
[45] A. Arendowski, J. Nizioł, K. Ossoliński, A. Ossolińska, T. Ossoliński, Z. Dobrowolski, T. Ruman, Laser desorption/ionization MS imaging of cancer kidney tissue on silver nanoparticle-enhanced target, Bioanalysis 10 (2018) 83–94, https://doi.org/10.4155/bio-2017-0195.
[46] D. Ackerman, S. Tumanov, B. Qiu, E. Michalopoulou, M. Spata, A. Azzam, H. Xie, M.C. Simon, J.J. Kamphorst, Triglycerides promote lipid homeostasis during hypoxic stress by balancing fatty acid saturation, Cell Rep. 24 (2018) 2596–2605, https://doi.org/10.1016/j.celrep.2018.08.015, e5.
[47] V. Tugnoli, A. Poerio, M.R. Tosi, Phosphatidylcholine and cholesteryl esters identify the infiltrating behaviour of a clear cell renal carcinoma: 1H, 13C and 31P MRS evidence, Oncol. Rep. 12 (2004) 353–356, https://doi.org/10.3892/or.12.2.353.